

Quadrupole Shift Cancellation Using Dynamic Decoupling

Ravid Shaniv, Nitzan Akerman, Tom Manovitz, Yotam Shapira, and Roei Ozeri

Department of Physics of Complex Systems, Weizmann Institute of Science, Rehovot 7610001, Israel



(Received 11 September 2018; published 5 June 2019)

We present a method that uses radio-frequency pulses to cancel the quadrupole shift in optical clock transitions. Quadrupole shifts are an inherent inhomogeneous broadening mechanism in trapped ion crystals and impose one of the limitations forcing current optical ion clocks to work with a single probe ion. Canceling this shift, at each interrogation cycle of the ion frequency, reduces the complexity in using $N > 1$ ions in clocks, thus allowing for a reduction of the instability in the clock frequency by \sqrt{N} according to the standard quantum limit. Our sequence relies on the tensorial nature of the quadrupole shift, and thus also cancels other tensorial shifts, such as the tensor ac stark shift. We experimentally demonstrate our sequence on three and seven $^{88}\text{Sr}^+$ ions trapped in a linear Paul trap, using correlation spectroscopy. We show a reduction of the quadrupole shift difference between ions to the ≈ 10 mHz level where other shifts, such as the relativistic second-order Doppler shift, are expected to limit our spectral resolution. In addition, we show that using radio-frequency dynamic decoupling we can also cancel the effect of first-order Zeeman shifts.

DOI: [10.1103/PhysRevLett.122.223204](https://doi.org/10.1103/PhysRevLett.122.223204)

Optical atomic clocks are one of the main achievements of quantum technology and provide some of the most accurate measurements to date, with applications ranging from basic science [1–3] to technology [4,5]. They operate at optical frequencies, using laser light as a local oscillator, which is locked to an atomic transition as a frequency reference.

Since the frequency reference is a two-level system, frequency interrogation is subject to quantum projection noise. According to the standard quantum limit, the signal to noise ratio of the experimental interrogation improves as \sqrt{N} when interrogating $N > 1$ atoms simultaneously. Multiple atomic frequency references are used e.g., in optical lattice clocks, where 10^4 or more neutral atoms are interrogated simultaneously [6].

Another class of optical clocks utilizes narrow optical transitions in ions, trapped in rf Paul traps [4,7]. These clocks offer excellent experimental control, long coherence times, long trapping lifetimes, and a fast duty-cycle for clock operation. However, trapping multiple ions in a linear chain can result in inhomogeneous shifts, e.g., relativistic Doppler shifts, magnetic field gradients, and quadrupole shifts. The latter arises because typically at least one of the ion levels has an electronic charge distribution that deviates from spherical symmetry by a leading quadrupole term. This charge distribution couples to electric field gradients at the ion's position, and leads to a clock transition frequency shift [8]. When a single ion is trapped, quadrupole shift arises primarily from trap dc electric field gradients. Typical shift values range between 10–100 Hz, much larger than the clock linewidth (1 Hz or below). When a multiple-ion crystal is trapped, the electric field gradient on

each ion results from both the trap electrodes and the crystal charge distribution, making it inhomogeneous. As a result, although multi-ion clocks have been proposed before [9–11], most ion optical clocks work with a single ion, limiting their averaging rate significantly.

Several techniques to mitigate the quadrupole shift in single ion clocks were developed [8,12,13], in which frequency measurements under different experimental parameters (e.g., orientation of the quantization magnetic field) are averaged, to give an average frequency with a null quadrupole shift contribution. However, in multiple ion clocks, these methods prove less useful due to the inhomogeneous nature of the quadrupole shift.

Another way to overcome the quadrupole shift is choosing ions with a small quadrupole moment. Examples include In^+ and Al^+ . However, these ions present different challenges, e.g., cooling transitions with UV wavelengths that are inaccessible to current laser technology [14–16].

Here, we introduce a Ramsey-like spectroscopy scheme, composed of two temporally separated $\pi/2$ optical pulses, preceding and terminating a radio-frequency (rf) sequence aimed at canceling the quadrupole shift at each clock interrogation. The measurement result of an interrogation cycle remains identical to the one in standard Ramsey spectroscopy, and the laser lock and other aspects are straightforward and described elsewhere. The aforementioned rf pulses produce a time-dependent Hamiltonian during the clock interrogation that relies on the quadrupole shift symmetry to cancel its effect. Furthermore, we show that it is also possible to cancel the first-order Zeeman shift using rf pulses. Our sequence can be considered as a continuous dynamical decoupling (DD) scheme [17,18].

Our method complements other Ramsey-like schemes aimed at reducing systematic shifts, see, e.g., Refs. [19,20].

In our model, we investigate an excited clock transition level with a total spin of $J > 1/2$, and an associated magnetic moment $\boldsymbol{\mu}_z = \gamma \mathbf{J}_z$ interacting with a local magnetic field $\vec{B} = B_z \hat{z}$. This spin evolves according to the free magnetic Hamiltonian $\mathcal{H}_m = \hbar \gamma B_z \mathbf{J}_z$. In the presence of an external electric field gradient across the ion position, a local quadrupole energy term is added: $\mathcal{H}_q = \hbar Q_J (\mathbf{J}^2 - 3\mathbf{J}_z^2)$, where Q_J contains the atomic level's quadrupole moment, the gradient of the electric field and geometric factors [8]. Our strategy for canceling quadrupole shifts relies on the identity $\mathbf{J}^2 - (\mathbf{J}_x^2 + \mathbf{J}_y^2 + \mathbf{J}_z^2) = 0$ and cancellation is therefore possible by spin J operators rotations. We note that these rotations are global operations applied uniformly on all ions, and are independent on the ion number.

To that aim, we add a control rf magnetic drive, which results in the Hamiltonian term $\mathcal{H}_c = 2\hbar \Omega(t) \cos(\omega_{\text{rf}} t - \phi) \mathbf{J}_x$, where $\omega_{\text{rf}} = (1/\hbar)\gamma B_z + \delta(t)$ is close to the Larmor frequency, $\Omega(t)$ is the multilevel Rabi frequency, and ϕ is the rf field phase. Moving to the interaction picture with respect to the drive and within the rotating wave approximation, we obtain the interaction Hamiltonian,

$$\mathcal{H}_{\text{int}}/\hbar = \delta(t) \mathbf{J}_z + Q_J (\mathbf{J}^2 - 3\mathbf{J}_z^2) + \Omega(t) [\cos(\phi) \mathbf{J}_x + \sin(\phi) \mathbf{J}_y]. \quad (1)$$

We assume that we can switch the rf drive on and off such that $\Omega(t)$ alternates between two values, $\Omega_0 \gg Q_J, \delta(t)$ and 0, and $\phi \in [0, 2\pi]$ is a controlled parameter. The quadrupole shift cancellation does not depend on the exact value of Ω_0 . We also assume that $\delta(t)$ varies slowly on the ion's interrogation time scale, and we approximate it as constant, $\delta(t) \approx \delta$. When the rf field is switched off for time τ , the spin evolves freely according to the evolution operator

$$F(\tau) = \exp \{i[\delta \tau \mathbf{J}_z + Q_J \tau (\mathbf{J}^2 - 3\mathbf{J}_z^2)]\}. \quad (2)$$

When short drive pulses are used, on timescales of $\tau \sim (\pi/\Omega_0)$, evolution due to the Hamiltonian terms $\delta \mathbf{J}_z + Q_J (\mathbf{J}^2 - 3\mathbf{J}_z^2)$ can be neglected, and the evolution is approximated as

$$\Pi^{\cos(\phi)x + \sin(\phi)y}(\Omega_0 \tau) = \exp [i\Omega_0 \tau (\cos(\phi) \mathbf{J}_x + \sin(\phi) \mathbf{J}_y)]. \quad (3)$$

Here, we introduced the pulse evolution operator $\Pi^d(\chi)$, where $d = \pm x, \pm y$ depending on ϕ , and χ is the rf pulse area. When $\tau \gg \pi/\Omega_0$, the evolution takes a different form. Assuming for example $\phi = \pm(\pi/2)$, the free evolution part in Eq. (1) can be written as the sum: $Q_J [\mathbf{J}^2 - \frac{3}{2}(\mathbf{J}_z^2 + \mathbf{J}_x^2)]$ and $\delta \mathbf{J}_z + Q_J [-\frac{3}{2}(\mathbf{J}_z^2 - \mathbf{J}_x^2)]$. While the first term commutes with the control operator $\Omega_0 \mathbf{J}_y$, the latter does not and

averages out. As a result, this continuous pulse evolution becomes,

$$\Pi^{\pm y}(\Omega_0 \tau) = \exp \left[i \left(Q_J \tau [\mathbf{J}^2 - \frac{3}{2}(\mathbf{J}_z^2 + \mathbf{J}_x^2)] \pm \Omega_0 \tau \mathbf{J}_y \right) \right], \quad (4)$$

where we used the same notation as for short pulses.

Our spectroscopy sequence for canceling the quadrupole shift is illustrated in Fig. 1. To match our experiment we describe our method explicitly using the example of a quadrupole allowed transition $|5S_{1/2}, m_S\rangle \leftrightarrow |4D_{5/2}, m_D\rangle$ in $^{88}\text{Sr}^+$ ion though it is valid for any choice of J other than $5/2$. Here, m_S and m_D are the corresponding Zeeman sublevels, and the overall Ramsey interrogation time is T . The sequence begins by initializing all ions in $|5S_{1/2}, m_S\rangle$. Next, an optical Ramsey $\pi/2$ pulse takes each ion to the superposition $\frac{1}{\sqrt{2}}(|5S_{1/2}, m_S\rangle + |4D_{5/2}, m_D\rangle)$. Following this pulse, a rf sequence is applied uniformly to all ions. This sequence takes the form of

$$F\left(\frac{T}{3}\right) \Pi^{-x}\left(\frac{\pi}{2}\right) \Pi^{-y}\left(\frac{\Omega_0 T}{3}\right) \Pi^y\left(\frac{\Omega_0 T}{3}\right) \Pi^x\left(\frac{\pi}{2}\right). \quad (5)$$

The first four operators correspond to a rf rotary echo [21] sequence, and the final operator is free evolution of the

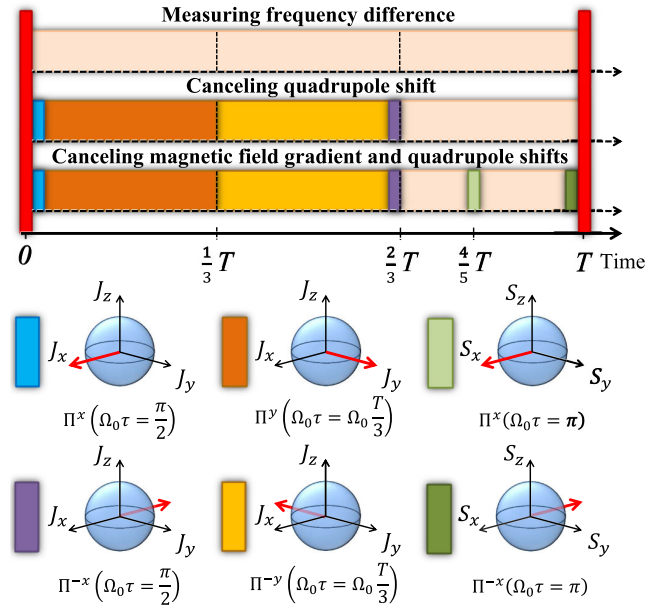


FIG. 1. Experimental sequences scheme. The sequence pulses are shown in different colors for different rf phases, different pulse times and different rf frequencies. In addition, a geometric representation legend for the angular momentum operators direction for each pulse is displayed. J_i represents pulses resonant with the excited large spin manifold, whereas S_i represents pulses resonant with the ground state. Red operations mark the opening and closing optical Ramsey $\pi/2$ pulses.

spin. Due to spectral separation, this sequence works primarily on the $|4D_{\frac{3}{2}}, m_D\rangle$ Zeeman manifold, and is exactly identical to $\exp\{i(\delta T/3\hbar)\mathbf{J}_z + (Q_J T/\hbar)[\mathbf{J}^2 - (\mathbf{J}_x^2 + \mathbf{J}_y^2 + \mathbf{J}_z^2)]\}$ (see Supplemental Material [22]). Since the right part in the argument is identically zero, we are left with $\exp[i(\delta T/3\hbar)\mathbf{J}_z]$, and the quadrupole shift term is eliminated. Since the tensor ac stark shift has a similar operator form as the quadrupole shift [8], our sequence cancels it as well. Finally, a second optical Ramsey $\pi/2$ pulse followed by state detection closes the Ramsey experiment. The residual frequency shift arising from the noncommuting terms neglected in Eq. (4) scales as $Q_j^k \delta^l / \Omega_0^2$ with integers k, l such that $k + l = 3$ (see Supplemental Material [22]). As an example, for $Q_J = \delta = 2\pi \times 10$ Hz and $\Omega_0 = 2\pi \times 50$ kHz the residual frequency shift would be smaller than $40 \mu\text{Hz}$.

We verified the cancellation of the quadrupole shift in an experiment with a three $^{88}\text{Sr}^+$ ion crystal trapped in a linear Paul trap. The optical quadrupole-allowed transition was addressed using a ≤ 20 Hz linewidth 674 nm laser, and the ions' state was detected using state-selective fluorescence detection on an EMCCD camera. Details of the experimental apparatus are found in the Supplemental Material [22] and in Ref. [23,24]. The axial trapping frequency was 1.5 MHz, resulting in a differential quadrupole shift between chain-edge and chain-middle ions of a few Hz for the $|4D_{\frac{3}{2}}, m_D\rangle$ state. Magnetic field of 0.3 mT splits the excited and ground states of the ion to their Zeeman manifolds. The rf DD sequence was implemented with $\Omega_0 = 2\pi \times 92$ kHz.

To avoid laser phase noise and ambient magnetic field drifts, we took advantage of the fact that the quadrupole shift is different between different ions, and used correlation spectroscopy to infer the frequency difference between transitions in different ions [25,26]. Here, at the end of the Ramsey sequence described above, the parity of the state, i.e., $P(DD) + P(SS) - P(SD) - P(DS)$ where P denotes probability and S (D) denotes states in the $|5S_{\frac{3}{2}}, m_s\rangle$ ($|4D_{\frac{3}{2}}, m_D\rangle$) manifold, was measured. Assuming full decoherence of the single ion local oscillator, this parity signal will oscillate at the absolute value of the frequency difference between the two ions, with half the fringe contrast (see the Supplemental Material [22]).

In order to measure the reduction in the quadrupole shift, we applied a magnetic field gradient, creating a large Zeeman shift difference between adjacent ions. Considering a chain of N ions, indexed from 1 to N along the trap axis, we denote by $\omega_{i,j} = |\omega_{i,j}^Q + \omega_{i,j}^M|$ the parity fringe frequency of ions i and j , where $\omega_{i,j}^Q$ and $\omega_{i,j}^M$ are its contributions due to quadrupole shift and magnetic field difference, respectively. Note that $\omega_{i,j} = \omega_{j,i}$. However, due to the fact that the quadrupole shift and Zeeman shift are symmetric and antisymmetric with respect to the chain center [see Fig. 2(a)] we can write $\omega_{i,j}^Q = \omega_{N+1-i, N+1-j}^Q$ and

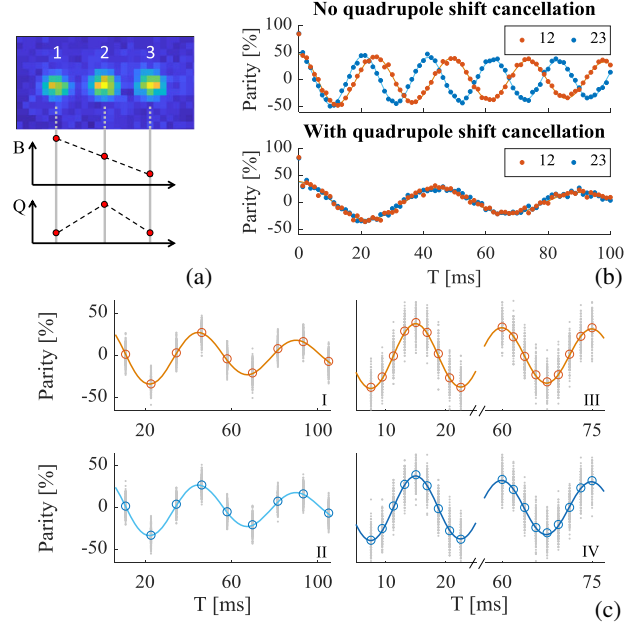


FIG. 2. Quadrupole shift cancellation results. (a) Three ions image on an EMCCD camera, along with position-dependent magnetic field (M) and quadrupole shift (Q). (b) Parity oscillations of ions (1,2) and (2,3) in orange and blue circles. Upper and lower plots correspond to Ramsey and quadrupole shift cancellation experimental sequences (see Fig. 1), respectively. The measured relative quadrupole shift is ~ 3.6 Hz. Here the chosen superposition was $\frac{1}{\sqrt{2}}(|5S_{\frac{3}{2}}, -\frac{1}{2}\rangle + |4D_{\frac{3}{2}}, -\frac{3}{2}\rangle)$. Upper and lower plots exhibit different mean parity frequency due to partial cancellation of Zeeman shifts in the DD sequence. (c) Quadrupole shift cancellation parity fringes with longer integration time. Frequencies were estimated by averaging frequencies from hundreds of minutes-long Ramsey experiments (Grey dots). (I,II) Parity fringes of (1,2) and (2,3) pairs, respectively, for the above superposition after integration of 20.5 hours. (III,IV) Parity fringes of (1,2) and (2,3) pairs, respectively, for $\frac{1}{\sqrt{2}}(|5S_{\frac{3}{2}}, -\frac{1}{2}\rangle + |4D_{\frac{3}{2}}, \frac{1}{2}\rangle)$ superposition, after integration of 14 hours. Empty circles are the average of all the data (grey points) and solid lines are maximum likelihood fits to the data, both exhibit similar frequencies agreement.

$\omega_{i,j}^M = -\omega_{N+1-i, N+1-j}^M$, and therefore we can conclude that $|\omega_{i,j} - \omega_{N+1-i, N+1-j}| = |2\omega_{i,j}^Q|$. Therefore, canceling the quadrupole shift means that the parity oscillation of ions (i,j) and $(N+1-i, N+1-j)$ coincide.

Our experimental results for three ions are shown in Fig. 2. As seen, with no quadrupole shift cancellation, frequency shift of ~ 3.6 Hz between ion pairs (1,2) and (2,3) is observed. With our DD sequence applied, the parity oscillations of the two pairs seem to coincide. A more quantitative measurement is shown in Fig. 2(c). Here parity fringes for ion pairs (1,2) and (2,3) with superposition $\frac{1}{\sqrt{2}}(|5S_{\frac{3}{2}}, -\frac{1}{2}\rangle + |4D_{\frac{3}{2}}, -\frac{3}{2}\rangle)$ are 22.146 ± 0.024 Hz and 22.168 ± 0.024 Hz, respectively, and therefore agree to within one standard deviation. For the

superposition $\frac{1}{\sqrt{2}}(|5S_{\frac{1}{2}}, -\frac{1}{2}\rangle + |4D_{\frac{3}{2}}, \frac{1}{2}\rangle)$, Parity fringes frequencies for ion pairs (1,2) and (2,3) are 66.722 ± 0.034 Hz and 66.768 ± 0.034 Hz, respectively, and they agree to 1.3 standard deviation, corresponding to relative quadrupole shift cancellation of less than 1×10^{-16} with respect to the optical transition frequency, limited by statistical uncertainty. We note, however, that since our trap has a significant axial micromotion gradient [27] we expect different ions to exhibit different measured frequency due to the relativistic Doppler effect [2,4]. We estimate these shifts along the trap axis to be in the 10s mHz scale. We therefore do not expect to verify the quadrupole shift cancellation better than this scale.

The experiment reported above was performed over the course of several weeks, not consecutively. Between one experiment and the next drifts in the frequency-matching between symmetric correlations (with respect to the chain center) were observed, up to 230 mHz. Although the source of these drifts is not fully identified, we believe they are not residual quadrupole shifts. First, the quadrupole shift in our lab is stable and changes by less than 10% over days. In addition, our DD cancellation method was identically repeated in different experimental realizations, and the residual quadrupole shift for our experimental parameters is expected to be less than 2 mHz (see Supplemental Material [22]). Therefore, residual quadrupole shifts cannot explain run-to-run variations in the symmetric correlations of 100s mHz. We note, however, that in these experiments we did not use mechanical shutters. The observed shifts could originate from differential light shifts from leaks of laser light during the interrogation time. Another possible systematic shift could arise from charging of the trap electrode surface from the presence of the violet Doppler cooling light which would lead to unwanted differential Doppler and Zeeman shifts.

Keeping quadrupole shift cancellation, additional rf pulses within the sequence can cancel the remaining first order Zeeman shifts from the last part of free evolution [28]. Here we apply rf π pulses that flip the two Zeeman states in the $|5S_{\frac{1}{2}}, m_S\rangle$ manifold during the final wait time as shown in Fig. 1. The pulse time is determined by taking into account the magnetic response of both excited and ground states. Figure 3 summarizes the experimental results for canceling both first-order Zeeman and quadrupole shifts on a seven-ion chain. As seen, following the cancellation sequence no apparent parity oscillations are observed, regardless of the correlation pair examined. We therefore conclude that both shifts are largely reduced.

Generally, the use of a dynamical sequence may increase sensitivity to noise spectral components at the sequence's frequency, including both external noise and noise in the DD pulses themselves. Here, as an example, the reduction in contrast is due to noisy magnetic field spectral components that overlap with our sequence. It can be reduced by appropriately minimizing this overlap, which in our case

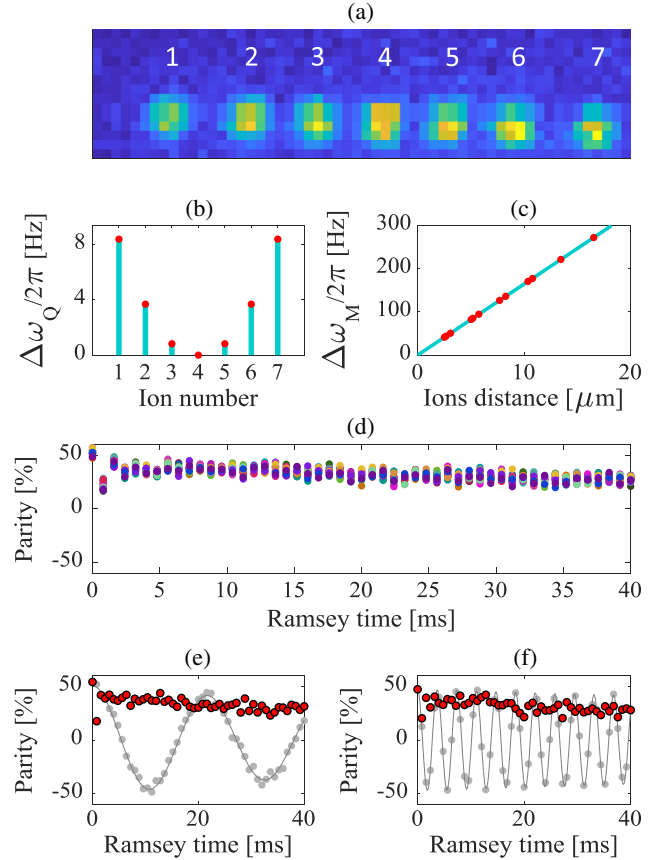


FIG. 3. Seven ions quadrupole shift and magnetic gradient cancellation experimental results. (a) Seven ion chain imaged on a EMCCD camera. (b) Relative quadrupole shift ($\Delta\omega_Q$) measurement. The shift (red circles) is relative to ion number 4, and it is given by $\frac{1}{2}||\omega_{i,4} - |\omega_{8-i,4}||$ for the i th ion frequency. (c) Magnetic field gradient shift ($\Delta\omega_M$) measurement. Ion distance is calculated from trap parameters, and the shift (red circles) is calculated as $\frac{1}{2}||\omega_{i,j} + |\omega_{8-i,8-j}||$. A linear fit (turquoise solid line) yields ≈ 16.4 Hz/ μm . Standard deviations for both (b) and (c) range from 60 to 130 mHz and therefore are too small to be presented. (d) Quadrupole and magnetic field gradient shifts cancellation experimental results, of all 21 correlations. (e),(f) Correlations (1,2) and (1,7) and their fit as examples for inhomogeneous shifts measurement experiment (grey circles and solid lines), respectively, along with their counterparts in the cancellation experiment.

would mean using a lower Rabi frequency (see Supplemental Material SM [22]).

Resonant rf drive applied on the excited state Zeeman separation is an off-resonance drive to the ground state Zeeman manifold. As a result, the latter's level spacing shifts are in analogy to the ac Stark shift. Taking as example a rf Rabi frequency on the ground state Zeeman transition of $\Omega_S \approx 2\pi \times 150$ kHz and detuning of $\delta_S \approx 3.5$ MHz the ground state levels will be shifted by $(\Omega_S^2/2\delta_S) = 2\pi \times 2.2$ kHz. This is a large unwanted shift originating from the cancellation sequence. In order to mitigate this shift, one could first choose a lower Rabi frequency, and

therefore reduce this shift quadratically. Another strategy uses the fact that the ground state levels are shifted symmetrically around the zero magnetic field energy. Two approaches can be taken. First, one could average measurements of two transitions with different m levels. For example, $|5S_{1/2}, \frac{1}{2}\rangle \leftrightarrow |4D_{3/2}, \frac{3}{2}\rangle$ and $|5S_{1/2}, -\frac{1}{2}\rangle \leftrightarrow |4D_{3/2}, -\frac{3}{2}\rangle$. This technique is widely used in current optical atomic clocks to eliminate first Zeeman shifts, but has the disadvantage of allowing magnetic field changes between interrogations. Second, additional rf pulses applied on the ground state Zeeman manifold can eliminate phase accumulation originating in such a symmetric shift, including magnetic field shifts and the shift mentioned above (see Supplemental Material [22]).

To conclude, in this Letter, we proposed and experimentally demonstrated a method to cancel quadrupole shifts in trapped ions systems. This shift poses a difficulty in the use of many ions in an ion-based optical atomic clock, and therefore canceling it allows for better signal to noise and more accurate and precise clock operation. The use of many-ion clock has additional challenges, including mitigating relativistic Doppler shifts, gradients in black body radiation shifts and ion-crystal lifetime in the trap. However, solutions have been proposed and demonstrated for this types of shifts, relying on ion-trap design and parameters choice [11,29]. Our sequence is based on rf pulses, which are experimentally easy to implement, and it complies with other proposed multi-ion clock designs and methods. Furthermore, we show that using these rf pulse sequences, magnetic field effects can be canceled as well. We used correlation spectroscopy as a tool for monitoring and verifying cancellation of multi-ion related shifts, and experimentally showed reduction of inhomogeneity from electric quadrupole interaction to below 1×10^{-16} , where statistical uncertainty as well as other systematic effects limit our resolution. We have demonstrated the cancellation of both quadrupole and magnetic field shifts in a seven-ion crystal; however our method will work equally well in a larger ion chain and may lead to a significant improvement in optical clock short term stability.

In parallel to our studies, a similar method that incorporates dynamic-decoupling techniques for the cancellation of quadrupole shifts was investigated [30].

This work was supported by the Crown Photonics Center, ICore-Israeli excellence center circle of light, the Israeli Science Foundation, the Israeli Ministry of Science Technology and Space, the Minerva Stiftung, and the European Research Council (consolidator Grant No. 616919-Ionology).

[1] S. Blatt, A. D. Ludlow, G. K. Campbell, J. W. Thomsen, T. Zelevinsky, M. M. Boyd, J. Ye, X. Baillard, M. Fouché, R. Le Targat *et al.*, New Limits on Coupling of Fundamental

- Constants to Gravity using ^{87}Sr Optical Lattice Clocks, *Phys. Rev. Lett.* **100**, 140801 (2008).
- [2] C.-W. Chou, D. B. Hume, T. Rosenband, and D. J. Wineland, Optical clocks and relativity, *Science* **329**, 1630 (2010).
- [3] R. M. Godun, P. B. R. Nisbet-Jones, J. M. Jones, S. A. King, L. A. M. Johnson, H. S. Margolis, K. Szymaniec, S. N. Lea, K. Bongs, and P. Gill, Frequency Ratio of Two Optical Clock Transitions in $^{171}\text{Yb}^+$ and Constraints on the Time Variation of Fundamental Constants, *Phys. Rev. Lett.* **113**, 210801 (2014).
- [4] A. D. Ludlow, M. M. Boyd, J. Ye, E. Peik, and P. O. Schmidt, Optical atomic clocks, *Rev. Mod. Phys.* **87**, 637 (2015).
- [5] C. Lisdat, G. Grosche, N. Quintin, C. Shi, S. M. F. Raupach, C. Grebing, D. Nicolodi, F. Stefani, A. Al-Masoudi, S. Dörscher *et al.*, A clock network for geodesy and fundamental science, *Nat. Commun.* **7**, 12443 (2016).
- [6] S. L. Campbell, R. B. Hutson, G. E. Marti, A. Goban, N. Darkwah Oppong, R. L. McNally, L. Sonderhouse, J. M. Robinson, W. Zhang, and B. J. Bloom *et al.*, A fermi-degenerate three-dimensional optical lattice clock, *Science* **358**, 90 (2017).
- [7] D. J. Wineland, C. Monroe, W. M. Itano, D. Leibfried, B. E. King, and D. M. Meekhof, Experimental issues in coherent quantum-state manipulation of trapped atomic ions, *J. Res. Natl. Inst. Stand. Technol.* **103**, 259 (1998).
- [8] W. M. Itano, External-field shifts of the $^{199}\text{Hg}^+$ optical frequency standard, *J. Res. Natl. Inst. Stand. Technol.* **105**, 829 (2000).
- [9] C. Champenois, M. Marciante, J. Pedregosa-Gutierrez, M. Houssin, M. Knoop, and M. Kajita, Ion ring in a linear multipole trap for optical frequency metrology, *Phys. Rev. A* **81**, 043410 (2010).
- [10] K. Arnold, E. Hajiyeve, E. Paez, C. Hui Lee, M. D. Barret, and J. Bollinger, Prospects for atomic clocks based on large ion crystals, *Phys. Rev. A* **92**, 032108 (2015).
- [11] J. Keller, T. Burgermeister, D. Kalincev, A. Didier, A. P. Kulosa, T. Nordmann, J. Kiethe, and T. E. Mehlstäubler, Controlling systematic frequency uncertainties at the 10^{-19} level in linear coulomb crystals, *Phys. Rev. A* **99**, 013405 (2019).
- [12] P. Dubé, A. A. Madej, J. E. Bernard, L. Marmet, J.-S. Boulanger, and S. Cundy, Electric Quadrupole Shift Cancellation in Single-Ion Optical Frequency Standards, *Phys. Rev. Lett.* **95**, 033001 (2005).
- [13] H. S. Margolis, G. P. Barwood, G. Huang, H. A. Klein, S. N. Lea, K. Szymaniec, and P. Gill, Hertz-level measurement of the optical clock frequency in a single $^{88}\text{Sr}^+$ ion, *Science* **306**, 1355 (2004).
- [14] E. Peik, G. Hollemann, and H. Walther, Laser cooling and quantum jumps of a single indium ion, *Phys. Rev. A* **49**, 402 (1994).
- [15] M. Eichenseer, A. Yu Nevsky, C. Schwedes, J. von Zanthier, and H. Walther, Towards an indium single-ion optical frequency standard, *J. Phys. B* **36**, 553 (2003).
- [16] P. O. Schmidt, T. Rosenband, C. Langer, W. M. Itano, J. C. Bergquist, and D. J. Wineland, Spectroscopy using quantum logic, *Science* **309**, 749 (2005).
- [17] F. F. Fanchini, J. E. M. Hornos, and R. d. J. Napolitano, Continuously decoupling single-qubit operations from a perturbing thermal bath of scalar bosons, *Phys. Rev. A* **75**, 022329 (2007).

- [18] G. Gordon, G. Kurizki, and D. A. Lidar, Optimal Dynamical Decoherence Control of a Qubit, *Phys. Rev. Lett.* **101**, 010403 (2008).
- [19] N. Huntemann, B. Lipphardt, M. Okhapkin, C. Tamm, E. Peik, A. V. Taichenachev, and V. I. Yudin, Generalized Ramsey Excitation Scheme with Suppressed Light Shift, *Phys. Rev. Lett.* **109**, 213002 (2012).
- [20] N. Huntemann, C. Sanner, B. Lipphardt, C. Tamm, and E. Peik, Single-Ion Atomic Clock with 3×10^{18} Systematic Uncertainty, *Phys. Rev. Lett.* **116**, 063001 (2016).
- [21] I. Solomon, Rotary Spin Echoes, *Phys. Rev. Lett.* **2**, 301 (1959).
- [22] See Supplemental Material at <http://link.aps.org/supplemental/10.1103/PhysRevLett.122.223204> for more experimental details and method's systematic shifts discussion.
- [23] N. Akerman, Y. Glickman, S. Kotler, A. Keselman, and R. Ozeri, Quantum control of $^{88}\text{Sr}^+$ in a miniature linear Paul trap, *Appl. Phys. B* **107**, 1167 (2012).
- [24] T. Manovitz, Individual addressing and imaging of ion in a Paul trap, Master's thesis, Feinberg Graduate School, The Weizmann Institute, 2016.
- [25] M. Chwalla, K. Kim, T. Monz, P. Schindler, M. Riebe, C. F. Roos, and R. Blatt, Precision spectroscopy with two correlated atoms, *Appl. Phys. B* **89**, 483 (2007).
- [26] C.-W. Chou, D. B. Hume, M. J. Thorpe, D. J. Wineland, and T. Rosenband, Quantum Coherence Between Two Atoms Beyond $Q = 10^{15}$, *Phys. Rev. Lett.* **106**, 160801 (2011).
- [27] N. Navon, S. Kotler, N. Akerman, Y. Glickman, I. Almog, and R. Ozeri, Addressing Two-Level Systems Variably Coupled to an Oscillating Field, *Phys. Rev. Lett.* **111**, 073001 (2013).
- [28] N. Akerman, N. Navon, S. Kotler, Y. Glickman, and R. Ozeri, Universal gate-set for trapped-ion qubits using a narrow linewidth diode laser, *New J. Phys.* **17**, 113060 (2015).
- [29] P. Dubé, A. A. Madej, Z. Zhou, and J. E. Bernard, Evaluation of systematic shifts of the $^{88}\text{Sr}^+$ single-ion optical frequency standard at the 10^{17} level, *Phys. Rev. A* **87**, 023806 (2013).
- [30] N. Aharon, N. Spethmann, I. D. Leroux, P. O. Schmidt, and A. Retzker, Robust optical clock transitions in trapped ions, [arXiv:1811.06732v1](https://arxiv.org/abs/1811.06732v1).